

# Reduction of Magnetic Field Inhomogeneity Artifacts in Echo Planar Imaging with SENSE and GESEPI at High Field

Qing X. Yang,<sup>1\*</sup> Jianli Wang,<sup>1</sup> Michael B. Smith,<sup>1,2</sup> Mark Meadowcroft,<sup>1</sup> Xiaoyu Sun,<sup>1</sup> Paul J. Eslinger,<sup>3</sup> and Xavier Golay<sup>4,5</sup>

**Geometric distortion, signal-loss, and image-blurring artifacts in echo planar imaging (EPI) are caused by frequency shifts and  $T_2^*$  relaxation distortion of the MR signal along the  $k$ -space trajectory due to magnetic field inhomogeneities. The EPI geometric-distortion artifact associated with frequency shift can be reduced with parallel imaging techniques such as SENSE, while the signal-loss and blurring artifacts remain. The gradient-echo slice excitation profile imaging (GESEPI) method has been shown to be successful in restoring tissue  $T_2^*$  relaxation characteristics and is therefore effective in reducing signal-loss and image-blurring artifacts at a cost of increased acquisition time. The SENSE and GESEPI methods are complementary in artifact reduction. Combining these two techniques produces a method capable of reducing all three types of EPI artifacts while maintaining rapid acquisition time. Magn Reson Med 52:1418–1423, 2004. © 2004 Wiley-Liss, Inc.**

**Key words:** fast imaging; image artifacts reduction;  $T_2^*$  contrast; EPI; high field MRI

Challenges to performing rapid echo planar imaging (EPI) at high field are increased considerably by amplified magnetic field inhomogeneity artifacts (1,2). Echo planar images are typically acquired with a long acquisition trajectory during which the MR signal is modulated by  $T_2^*$  relaxation. This makes EPI inherently vulnerable to magnetic field inhomogeneity, which is most noticeable in images of the inferior and frontal brain areas. Given the important role of EPI in dynamic imaging, significant efforts have been made in developing techniques to reduce or eliminate these artifacts (3–31).

The magnetic field inhomogeneity artifacts include signal loss, image blurring, and geometric distortion. Among these artifacts, image blurring and signal loss are caused by distortion of  $T_2^*$  relaxation predominantly due to the

through-plane local gradient, while geometric distortion is caused by a frequency shift of the MR signal due to the in-plane local gradient. Since the gradient-echo slice excitation profile imaging (GESEPI) method has been shown to be capable of removing distortions in  $T_2^*$  relaxation characteristics caused by the through-plane local gradient at high field strengths (13,31), it can be highly effective in correcting EPI signal-loss and image-blurring artifacts. While GESEPI provides excellent reduction of these two kinds of artifacts, its utility for rapid EPI is limited by increased image acquisition time. This limitation can be overcome with SENSE encoding, which reduces  $k$ -space sampling time (32). In addition, the geometric distortion artifact associated with the in-plane local gradient is significantly mitigated with SENSE as a result of reduced data acquisition time (33–35). The signal-loss and image-blurring artifacts associated with the through-plane local gradient, however, still remain in SENSE EPI. Thus, incorporation of SENSE with GESEPI will provide a more effective method for correcting all three types of artifacts while reducing image acquisition time. In this paper, a SENSE-GESEPI approach is introduced for acquiring artifact-free, heavily  $T_2^*$ -weighted echo planar images of the brain at a field strength of 3.0 T. A theoretical analysis of artifact reduction with GESEPI and SENSE in EPI acquisition is provided. To validate the theoretical analysis, experimental results of artifact reductions with SENSE, GESEPI, and SENSE-GESEPI in EPI are systematically evaluated with phantom and in vivo human studies.

## THEORY

The effects of local magnetic field gradients on EPI can be decomposed into through-plane and in-plane components and treated separately. The through-plane local gradient plays a dominant role in distortion of tissue-specific  $T_2^*$  relaxation characteristics (3,6,9,31). Assuming that magnetic field inhomogeneity in the slice-selection direction,  $z$ , can be approximated with a linear local gradient,  $G_1$ , voxel signal intensity during a two-dimensional (2D) EPI acquisition can be described as

$$S = M_0 \exp(-t/T_2^*) \text{sinc}[\gamma G_1 z_0 t/2], \quad [1]$$

where  $\gamma$  is the gyromagnetic ratio,  $M_0$  is the magnetization density, and  $z_0$  is the excited slab thickness (13). In the above expression, an ideal excitation profile is assumed. The  $T_2^*$  decay during data acquisition time,  $t$ , is distorted by  $G_1$  with a sinc-function modulation. Distortion of  $T_2^*$  relaxation characteristics results in a strong attenuating

<sup>1</sup>Department of Radiology (Center for NMR Research), Pennsylvania State University College of Medicine, Milton S. Hershey Medical Center, Hershey, Pennsylvania.

<sup>2</sup>Department of Cellular and Molecular Physiology, Pennsylvania State University College of Medicine, Milton S. Hershey Medical Center, Hershey, Pennsylvania.

<sup>3</sup>Departments of Neurology, Behavioral Science, and Pediatrics (Laboratory of Clinical Neuropsychology and Cognitive Neuroscience), Pennsylvania State University College of Medicine, Milton S. Hershey Medical Center, Hershey, Pennsylvania.

<sup>4</sup>Department of Radiology, Johns Hopkins University, Baltimore, Maryland.

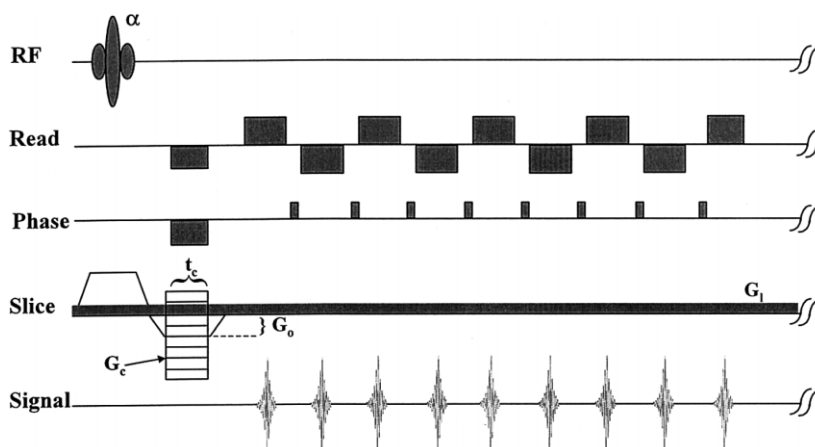
<sup>5</sup>F. M. Kirby Research Center, Kennedy Krieger Institute, Baltimore, Maryland. Grant sponsor: NIH Bioengineering Research Partnerships; Grant number: RO1 EB00454–01A1.

\*Correspondence to: Qing X. Yang, Department of Radiology (Center for NMR Research), M. S. Hershey Medical Center, 500 University Drive, Hershey, PA 17033. E-mail: qyang@psu.edu

Received 23 February 2004; revised 5 August 2004; accepted 5 August 2004. DOI 10.1002/mrm.20303

Published online in Wiley InterScience (www.interscience.wiley.com).

FIG. 1. Timing diagram of the GESEPI EPI method.  $G_1$  represents the local field gradient.  $G_c$  and  $G_o$  are compensation and slice rewinding gradients, respectively.  $G_c$  is varied in  $N$  equal incremental steps. The local gradient, although relatively small in strength, exerts a dephasing effect on the MR signal during the entire readout period. Multifold decrease in readout time with the SENSE encoding technique facilitates artifact reduction with the GESEPI method.



modulation of the MR signal along EPI  $k$ -space trajectory, causing signal-loss and image-blurring artifacts.

As shown in the timing diagram in Fig. 1, to remove the local gradient modulation on voxel signal, the GESEPI technique acquires multiple ( $N$ ) images with an incremental compensation gradient,  $G_c$ , in the slice-selection direction (13). In this case, signal intensity of a voxel in the excited slab is expressed in  $k$ -space as

$$S = M_0 \exp(-t/T_2^*) \text{sinc}[\pi(k_c - k_1(t))z_0], \quad [2]$$

where  $k_c = \gamma G_c \tau/2\pi$ ,  $k_1 = \gamma G_1 t/2\pi$ , and  $\tau$  represents the duration of  $G_c$ . Applying Fourier transform to Eq. [2] with respect to  $k_c$  yields a set of images of  $N$  subslices with intensity,  $I$ , given by

$$I = M_0 \exp(-t/T_2^*) \exp[i\gamma G_1 z_0 t] \text{rect}(N), \quad [3]$$

where  $\text{rect}$  is a rectangular function representing the pixel intensity profile of the excited slab. The sinc-function modulation on  $T_2^*$  relaxation in Eq. [1] is replaced with a phase modulation that does not affect the magnitude image. By removal of the sinc-function modulation due to  $G_1$  during EPI acquisition, GESEPI recovers signal loss and reduces image blurring.

Since  $G_c$  is, effectively, also a phase-encoding gradient in the slice direction, the GESEPI technique can be regarded as an oversampled three-dimensional (3D) acquisition of the excited slab consisting of  $N$  subslices. The images of the subslices in the oversampled region are discarded, because they are outside the excited slab with no appreciable signal intensity. Subsequently, the remaining magnitude images of adjacent subslices are added in groups to yield a set of final images with the desired slice thickness.

The frequency shift of the MR signal by in-plane local gradient, on the other hand, results in pixel shift and distortion in EPI. These artifacts are more prominent in the phase-encoding direction, because the encoding gradient and effective spectral bandwidth in this direction are relatively small and, thus, more susceptible to local field gradients and resultant frequency-shift perturbations. One solution to alleviate in-plane local gradient artifacts is to increase phase-encoding gradient strength and decrease

image acquisition time. This solution is the natural consequence of SENSE acquisition, in which case the phase-encoding gradient is increased by SENSE reduction factor,  $r$ , while acquisition time is reduced by the same factor. Thus, those artifacts caused by the in-plane local gradient are significantly reduced with SENSE. Taken together, GESEPI and SENSE are complementary methods, allowing for reduction of EPI artifacts due to both in- and through-plane gradients.

## METHODS

To experimentally demonstrate the theoretical analysis of voxel signal intensity behavior along  $k$ -space trajectory and deblurring effect of the GESEPI method for EPI, a study using a quasi-point source phantom, shown in Fig. 2, was first carried out. This phantom consisted of two 5-mm-diameter tubes filled with gelatin, with a 1.8-mm distance between the tubes. The tubes were aligned with the  $B_0$  field, serving as quasi-point sources for axial images. This phantom is simply termed “point source” hereafter for brevity. Standard gradient-echo (GE) and GESEPI echo planar images were acquired on a MedSpec S300 whole-body imager (Bruker Biospin Corp., Ettlingen, Germany) from two axial slices: Slice I was located 37 mm from the gelatin–air interface where local gradients were

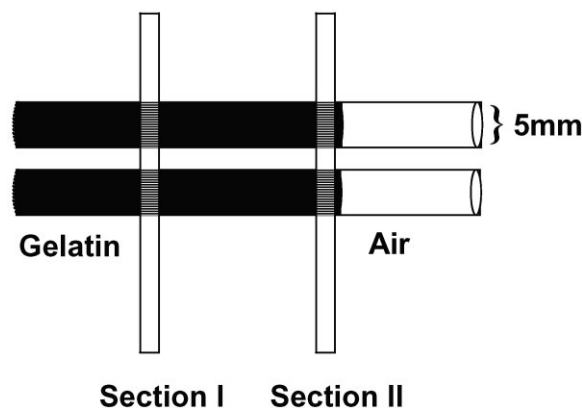


FIG. 2. Experimental setup for the point source phantom study.

absent, and Slice II was located 2 mm from the gelatin–air interface where strong local field gradients were present. For each slice, two sets of standard GE and GESEPI echo planar images were acquired with and without phase-encoding gradient in the left–right direction. In addition, evaluation of signal-loss artifact reduction with SENSE-GESEPI was carried out with a susceptibility phantom. The susceptibility phantom consisted of a 16-cm water sphere with a 3-cm-diameter air-filled plastic ball suspended in the center to simulate air-containing structures in the human head. The GESEPI EPI phantom images were acquired on a 3.0 T Intera system (Philips Medical Systems, The Netherlands) with an effective TE = 48.3 msec, TR = 5000 msec, receiver bandwidth = 142 kHz, field of view (FOV) =  $25 \times 25$  cm<sup>2</sup>, matrix =  $128 \times 128$  and slice thickness = 5 mm in 16 equal incremental compensation gradient steps. Standard GE and spin-echo (SE) echo planar images with the same acquisition parameters were also obtained for comparison purposes.

For human studies, the echo planar images with SENSE-GESEPI and standard SENSE were acquired from human brains on a 3.0 T Intera system. SENSE-GESEPI EPI axial images were acquired from seven axial slabs with thickness of 8 mm, TR = 297 msec, effective TE = 30 msec, FA = 40°, receiver bandwidth = 184 kHz, FOV =  $21 \times 21$  cm<sup>2</sup>, matrix =  $80 \times 80$  (zero-filled and reconstructed to  $128 \times 128$ ), NEX = 1. With 10  $G_c$  steps, acquisition time/volume = 3.0 sec. With SENSE reduction factor,  $r = 3$ , the acquisition window for each single-shot image was 30 msec. Three-dimensional Fourier transforms were performed on the data from each excited slab, generating a total of 70 subslices. After the 2 subslices on each side of the excited slabs in the oversampled region were discarded (14 subslices total), 14 slices with 4-mm thickness were obtained by adding every 4 adjacent subslice images. For comparison purposes, standard SE and GE SENSE echo planar images of 14 axial slices were acquired from the same brain volume with slice thickness = 4 mm, TR = 3 sec, effective TE = 30 msec, FA = 90°, FOV =  $21 \times 21$  cm<sup>2</sup> and matrix =  $80 \times 80$ . Informed consent approved by the Institutional Review Board was obtained from each human subject enrolled in this study.

## RESULTS

To demonstrate blurring artifact reduction by the GESEPI method, Fig. 3 shows a comparison of echo planar images acquired with and without application of the GESEPI technique from two separate slices of the point source phantom. The three images in Fig. 3a were obtained without a phase-encoding gradient in the left–right direction. These images are projection images from the point-source phantom. The plot in Fig. 3b under each image represents the signal intensity profile from the same horizontal line passing through one of the point sources in the image. Since no phase-encoding gradient was applied, the image intensity distributions along this direction were determined by  $T_2^*$  relaxation characteristics only. Therefore, each plot represents a profile of the point spread function (PSF) along the horizontal direction using the corresponding acquisition method. The echo planar image signal intensity profile in the homogeneous region of Slice I yields a sharp peak as

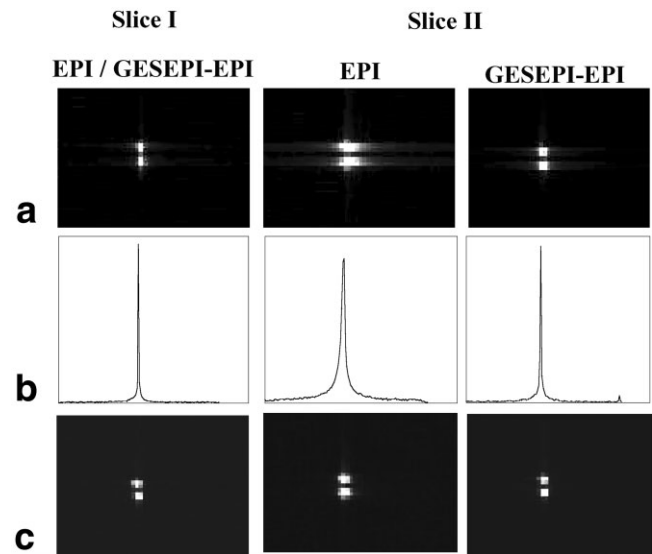


FIG. 3. Images acquired without phase-encoding in the left–right direction (a), intensity profiles through one of the point sources (b), and the corresponding images with phase-encoding. The linewidths (FWHM) of the plots are 0.71 pixels for Slice I and 3.5 pixels for Slice II. The GESEPI method reduced the linewidth in Slice II to 1.2 pixels. The images acquired with phase-encoding in (c) show a reduction of the blurring artifact in EPI using the GESEPI method. Image intensities in (a) were adjusted to facilitate visualization of PSF.

expected, rendering a well-defined PSF. Assuming the plot is a single Lorentzian, the linewidth (FWHM) is 0.71 pixel wide. In the inhomogeneous region near the gelatin–air interface in Slice II, however, the signal intensity spreads out into the entire FOV in the horizontal direction, representing a broad PSF. The corresponding linewidth is 3.5 pixels wide. The image resolution under such a condition is significantly compromised. The PSF profile in the same slice of the GESEPI echo planar image is significantly improved as its linewidth is reduced to 1.2 pixels. Figure 3c shows the actual EPI and GESEPI-EPI images of the point-source phantom of corresponding slices. The blurring artifact due to the local field gradient and its reduction with GESEPI can be seen clearly in the corresponding images.

Figure 4 shows four sets of echo planar axial images of the same volume from the susceptibility phantom with the first slice (left-most column) cutting through the edge of the air sphere in the phantom. The images in the first row were acquired using the GE method without SENSE ( $r = 1$ ), and the remaining rows were obtained with SENSE ( $r = 3$ ) using GE, GESEPI, and SE methods, respectively, as indicated on the left side of each row. The diminishing dark region found in the image center of the first row as the slices move away from the air sphere is a typical signal-loss artifact in GE echo planar images produced by the local field gradient. Comparing these images with corresponding images acquired with SENSE in the second row, the signal-loss artifact remains but with a different appearance as the SENSE factor increases to 3. The artifact in the images in the third row taken with the SENSE-GESEPI method is significantly reduced, yielding similar image intensity distributions to that with the SE method in the bottom row.

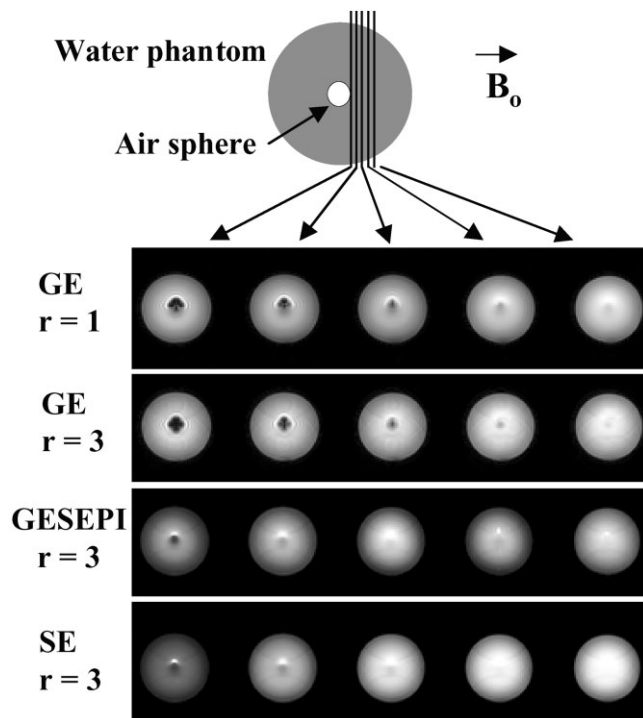


FIG. 4. The susceptibility phantom and echo planar images from five axial slices of the phantom acquired using GE without SENSE ( $r = 1$ ), with SENSE ( $r = 3$ ), GESEPI with SENSE ( $r = 3$ ), and SE with SENSE ( $r = 3$ ) methods. The slice of the images on the left column was cut axially through the edge of the air sphere. Signal-loss artifact in the center of the standard GE echo planar images appears stronger with increasing SENSE reduction factor.

Figure 5 shows two sets of axial human brain GE echo planar images acquired without SENSE and with SENSE ( $r = 3$ ). To assess the geometrical distortion artifact, identical ellipses were drawn around the contour of the brain in images acquired from a specific brain slice with and without SENSE. The image of this slice without SENSE exhibits a typical EPI geometrical-distortion artifact, characterized by the anterior brain area being stretched outside the ellipse, due to the local field gradient around the frontal sinus. As previously demonstrated (33–35), this artifact was significantly reduced with the SENSE method. Similar to the susceptibility phantom results in Fig. 4, the signal-loss artifacts as indicated by arrows remain pronounced in the images with SENSE with altered appearance. Thus, while the SENSE technique is effective in reducing geometrical distortion due to the in-plane local gradient, it is ineffective in reducing signal-loss artifact due to the through-plane local gradient.

Figure 6 shows three sets of echo planar images from a human brain acquired using GE, GESEPI, and SE methods with SENSE ( $r = 3$ ). As indicated by the arrows, severe signal-loss artifacts in the inferior–frontal and temporal brain regions can be seen in all slices acquired with the GE method. Thus, the signal-loss artifact remains a serious problem for  $T_2^*$  brain imaging with SENSE at 3.0 T. As seen in Fig. 6b, complimentary to the SENSE method, the GESEPI technique significantly reduces the signal-loss artifact. The effectiveness of sig-

nal-loss artifact reduction can be seen when comparing these with corresponding SE images. Incorporation of GESEPI with SENSE allows for effective reduction of all three types of artifacts in EPI.

## DISCUSSION

Signal-loss and image-blurring artifacts occur concomitantly in  $T_2^*$ -weighted echo planar images because both artifacts are caused by  $T_2^*$  relaxation distortion due to the through-plane local field gradient. It is important to recognize, however, that a method to remove the signal-loss artifact does not necessarily remove the image-blurring artifact in EPI. For example, methods of adding multiple magnitude images acquired with different strengths of the slice-refocusing gradient result in a stronger image-blurring artifact. This is because the refocusing gradient utilized in these techniques only compensates the MR signal phase dispersion occurring at the center of  $k$ -space while modulation by the distorted  $T_2^*$  remains along the rest of EPI  $k$ -space trajectory. The composite image obtained by adding magnitude images acquired with different refocusing gradients would evidently inherit the blurring artifacts of all its component images. As shown theoretically and demonstrated experimentally with the phantoms, the GESEPI technique is capable of correcting both artifacts. In addition, signal-noise-ratio (SNR) is reduced in the composite images obtained by summing magnitude images acquired with different refocusing gradients. The reason

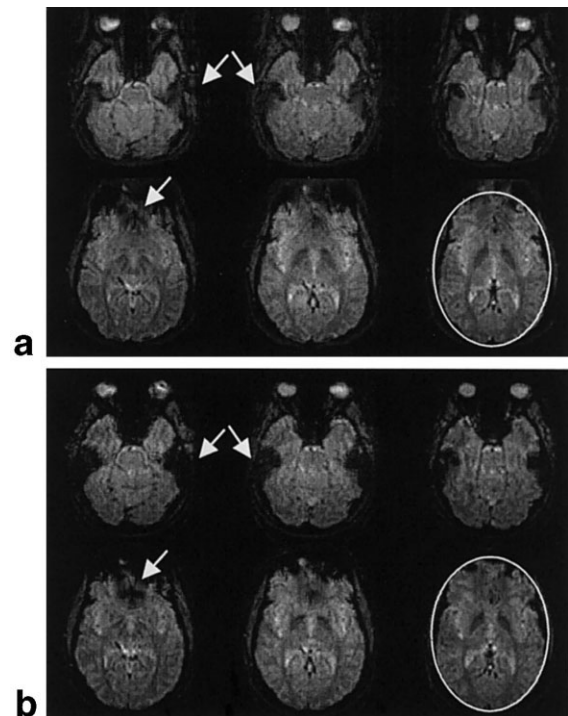


FIG. 5. GE echo planar images acquired from the same human brain volume without SENSE (a) and with SENSE ( $r = 3$ ) (b). To facilitate visual assessment of geometrical distortions in the images, identical ellipses were superimposed on the bottom right images. The arrows indicate the typical signal-loss artifact in the inferior–frontal and temporal brain regions.

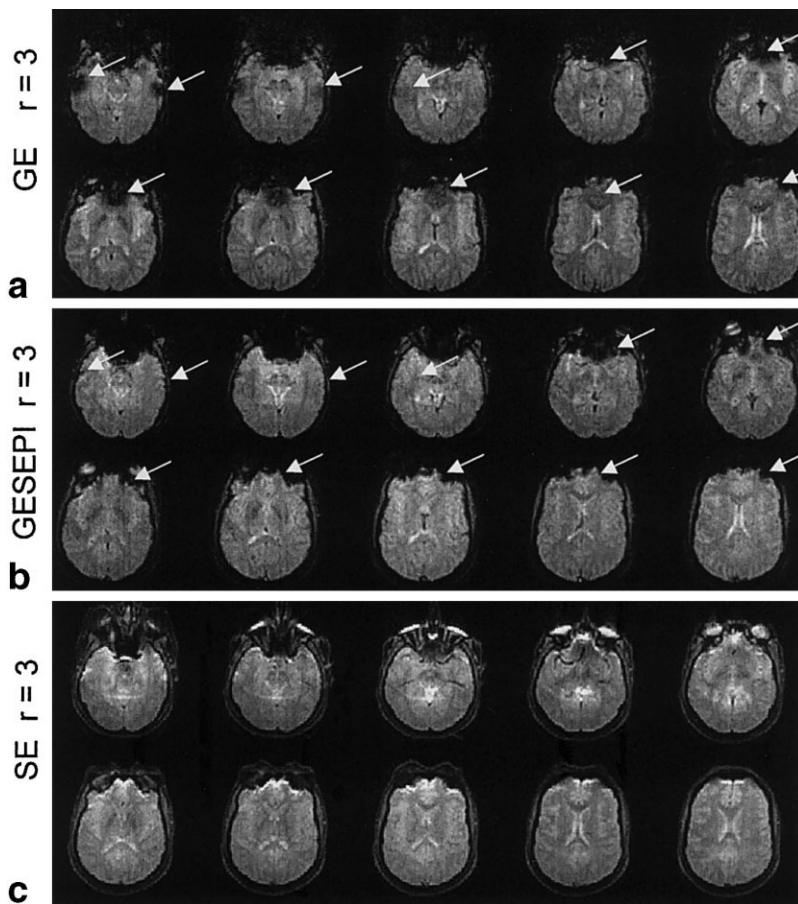


FIG. 6. Echo planar images acquired from the same human brain volume with SENSE ( $r = 3$ ) using GE (a), GESEPI (b), and SE (c) methods. Typical signal-loss artifact in the GE images (a) in the inferior frontal and temporal brain regions indicated by the arrows is reduced significantly with GESEPI (b).

for this is that image pixel intensities acquired with different refocusing gradients are maximum only when  $k_c = k_1$  such that these images contain only different parts of the object in the same slice according to the strength of the local field gradient (3,10). Summing these magnitude images results in no signal-averaging enhancement but adds noise to the signal. As shown in Eq. [2], the GESEPI technique removes sinc-function modulation by the local field gradient on the  $k$ -space signal. Subsequently, the signals acquired with multiple  $G_c$  steps are properly integrated with a Fourier transform. The SNR of a given slice is maintained.

The phantom and human brain data presented demonstrate that the SENSE and GESEPI methods are complementary and mutually facilitating in artifact reduction. Combining these two techniques allows for effective correction of all three kinds of artifacts in echo planar images. As discussed in theory, the artifacts in EPI caused by static field inhomogeneity can be classified into two categories and addressed using different approaches. While signal-loss and image-blurring artifacts caused by the through-plane local gradient can be effectively reduced with the GESEPI method, the geometric-distortion artifact caused by the in-plane local gradient remains uncorrected. Conversely, the SENSE method is effective in reducing the geometric distortion but ineffective in correcting the signal-loss and image-blurring artifacts. When combined with the SENSE encoding technique, the GESEPI method is more effective in reducing signal-loss and image-blur-

ring artifacts because of the reduction of readout time. In addition, the limitation of increased image acquisition time for GESEPI is addressed efficiently with SENSE, allowing acquisition of artifact-corrected images of the brain in under 3 sec. Therefore, SENSE-GESEPI is a method of choice for high field  $T_2^*$  EPI applications.

In the GESEPI method, TR and flip angle are reduced in order to maintain image acquisition speed for dynamic applications. This would lead to SNR reduction. However, the SNR reduction due to shortened TR and the use of smaller flip angle is offset by a multiple-fold increase in slab thickness. Our experimental results from both phantom and in vivo studies indicate that the SNR of GESEPI is comparable to standard echo planar images of the same slice thickness. Our results are consistent with the theoretical analysis on SNR comparison between 2D and 3D imaging methods involving steady-state data acquisition (15). In practice, optimal imaging parameters such as TR,  $N$ , and slab thickness for SENSE-GESEPI should be determined by the tradeoffs among SNR, artifact reduction, image acquisition speed, and spatial resolution (final image slice thickness) required by a specific application. Thus, a systematic investigation is necessary to further address these practical issues.

Although  $T_2^*$  contrast imaging is widely used, effective utilization of  $T_2^*$  contrast for scientific and clinical investigations has been limited by static magnetic field inhomogeneity artifacts. Magnetic field inhomogeneity can be produced by imperfect static field adjustments (shimming)

and unavoidable local field gradients near the air-filled structures inside the human head. For the later case, the regions influenced by the susceptibility artifacts are associated with many important brain functions with broad clinical implications. To remove field inhomogeneity in these brain regions with shimming is difficult. Thus, SENSE-GESEPI addresses a critical issue for performing rapid imaging at high field strength. Furthermore, since the EPI  $k$ -space signal of SE is also modulated with  $T_2^*$  relaxation, the associated blurring artifact exists in SE echo planar images and becomes aggravated at higher field strengths. Therefore, the SENSE-GESEPI method may be used for reductions of artifacts in SE EPI at high field.

In conclusion, we have demonstrated the effectiveness of the SENSE-GESEPI method in reducing artifacts in EPI. This method addresses an important problem for  $T_2^*$  dynamic imaging at high field strengths, allowing for acquisition of reliable  $T_2^*$  contrast echo planar images with effective removal of all three types of field inhomogeneity artifacts. Thus, the SENSE-GESEPI method is a valuable tool for dynamic studies with EPI at high field strength.

## ACKNOWLEDGMENTS

We thank Dr. Peter C. M. van Zijl for his insightful discussions and the assistance in conducting the experiments at the F. M. Kirby Research Center for Functional Brain Imaging of the Kennedy Krieger Institute.

## REFERENCES

- Abduljalil AM, Robitaille PM. Macroscopic susceptibility in ultra high field MRI. *J Comput Assist Tomogr* 1999;23:832–841.
- Yang QX, Smith MB, Zhu X, Liu H, Michaeli S, Zhang X, etc.  $T_2^*$ -weighted human brain imaging with the GESEPI at 7.0 Tesla. In: Proceedings of the 8th Annual Meeting of ISMRM, Denver, 2000. p 1684.
- Frahm J, Merboldt KD, Hänicke W. Direct FLASH MR imaging of magnetic field inhomogeneities by gradient compensation. *Magn Reson Med* 1988;6:474–480.
- Haacke EM, Tkach JA, Parrish TB. Reduction of  $T_2^*$  dephasing in gradient field-echo imaging. *Radiology* 1989;170:457–462.
- Cho ZH, Ro YM. Reduction of susceptibility artifact in gradient-echo imaging. *Magn Reson Med* 1992;23:193–200.
- Ordidge RJ, Gorell JM, Deniau JC, Knight RA, Helpert JA. Assessment of relative brain iron concentrations using  $T_2$ -weighted and  $T_2^*$ -weighted MRI at 3 Tesla. *Magn Reson Med* 1994;32:335–341.
- Yablonskiy DA, Haacke EM. Theory of NMR signal behavior in magnetically inhomogeneous tissues: the static dephasing regime. *Magn Reson Med* 1994;32:749–763.
- Frahm J, Merboldt KD, Hänicke W. The effects of intravoxel dephasing and incomplete slice refocusing on susceptibility contrast in gradient-echo MRI. *J Magn Reson B* 1995;109:234–237.
- Ro YM, Cho ZH. Susceptibility magnetic resonance imaging using spectral decomposition. *Magn Reson Med* 1995;33:521–528.
- Constable RT. Functional MR imaging using gradient-echo echo-planar imaging in the presence of large static field inhomogeneities. *J Magn Reson Imaging* 1995;5:746–752.
- Yang QX, Dardzinski BJ, Li S, Smith MB. Multi-gradient echo with susceptibility inhomogeneity compensation (MGESIC): demonstration of fMRI in the olfactory cortex at 3.0 T. *Magn Reson Med* 1997;37:331–335.
- Chen NK, Wyrwicz AM. Removal of introvoxel dephasing artifact in gradient-echo images using a field-map based RF refocusing technique. *Magn Reson Med* 1999;42:807–812.
- Yang QX, Williams GD, Demeure RJ, Mosher TJ, Smith MB. Removal of local field gradient artifacts in  $T_2^*$ -weighted images at high fields by gradient-echo slice excitation profile imaging. *Magn Reson Med* 1998;39:402–409.
- Yang QX, Edmister WB, Kwong KK, Demeure RJ, Smith MB. Removal of the signal-loss artifacts in  $T_2^*$ -weighted EPI. In: Proceedings of the 6th Annual Meeting of ISMRM, Sydney, Australia, 1998. p 1443.
- Glover GH. 3D z-shim method for reduction of susceptibility effects in BOLD fMRI. *Magn Reson Med* 1999;42:290–299.
- Stenger VA, Boada FE, Noll DC. Three-dimensional tailored RF pulses for the reduction of susceptibility artifacts in  $T_2^*$ -weighted functional MRI. *Magn Reson Med* 2000;44:525–531.
- Fernandez-Seara MA, Wehrli FW. Postprocessing technique to correct for background gradients in image-based  $R_2^*$  measurements. *Magn Reson Med* 2000;44:358–366.
- Merboldt KD, Finsterbusch J, Frahm J. Reducing inhomogeneity artifacts in functional MRI of human brain activation-thin sections vs gradient compensation. *J Magn Reson* 2000;145:184–191.
- Yang Y, Gu H, Zhan W, Xu S, Silbersweig DA, Stern E. Simultaneous perfusion and BOLD imaging using reverse spiral scanning at 3T: characterization of functional contrast and susceptibility artifacts. *Magn Reson Med* 2002;48:278–289.
- Yang Q, Stenger V, Smith MB, Boada F, Noll D. Reduction of the blurring artifacts due to the local field inhomogeneity in spiral imaging. In: Proceedings of the 9th Annual Meeting of ISMRM, Glasgow, Scotland, 2001. p 741.
- Glover GH, Law CS. Spiral in/out BOLD fMRI for increased SNR and reduced susceptibility artifacts. *Magn Reson Med* 2001;46:515–522.
- Schmithorst VJ, Dardzinski BJ, Holland SK. Simultaneous correction of ghost and geometric distortion artifacts in EPI using a multiecho reference scan. *IEEE Trans Med Imaging* 2001;20:535–539.
- Wild JM, Martin WR, Allen PS. Multiple gradient echo sequence optimized for rapid, single-scan mapping of  $R_2^*$  at high  $B_0$ . *Magn Reson Med* 2002;48:867–876.
- Gu H, Feng H, Zhan W, Xu S, Silbersweig DA, Stern E, Yang Y. Single-shot interleaved z-shim EPI with optimized compensation for signal losses due to susceptibility-induced field inhomogeneity at 3 T. *Neuroimage* 2002;17:1358–1364.
- Li Z, Wu G, Zhao X, Luo F, Li SJ. Multiecho segmented EPI with z-shimmed background gradient compensation (MESBAC) pulse sequence for fMRI. *Magn Reson Med* 2002;48:312–321.
- Wilson JL, Jenkinson M, Jezzard P. Protocol to determine the optimal intraoral passive shim for minimisation of susceptibility artifact in human inferior frontal cortex. *Neuroimage* 2003;19:1802–1811.
- Deichmann R, Gottfried JA, Hutton C, Turner R. Optimized EPI for fMRI studies of the orbitofrontal cortex. *Neuroimage* 2003;19:430–441.
- Posse S, Shen Z, Kiselev V, Kemna LJ. Single-shot  $T_2^*$  mapping with 3D compensation of local susceptibility gradients in multiple regions. *Neuroimage* 2003;18:390–400.
- de Zwart JA, van Gelderen P, Kellman P, Duyn JH. Application of sensitivity-encoded echo-planar imaging for blood oxygen level-dependent functional brain imaging. *Magn Reson Med* 2002;48:1011–1020.
- Weiger M, Pruessmann KP, Osterbauer R, Bornert P, Boesiger P, Jezzard P. Sensitivity-encoded single-shot spiral imaging for reduced susceptibility artifacts in BOLD fMRI. *Magn Reson Med* 2002;48:860–866.
- Yang QX, Dardzinski BJ, Demeure RJ, Briggs RW, Smith MB. Removal of local field gradient artifacts in  $T_2^*$  measurement and  $T_2^*$  contrast at high field. In: Proceedings of the 6th Annual Meeting of ISMRM, Sydney, Australia, 1998. p 578.
- Pruessmann KP, Weiger M, Scheidegger MB, Boesiger P. SENSE: sensitivity encoding for fast MRI. *Magn Reson Med* 1999;42:952–962.
- Bammer R, Keeling SL, Augustin M, Pruessmann KP, Wolf R, Stollberger R, Hartung HP, Fazekas F. Improved diffusion-weighted single-shot echo-planar imaging (EPI) in stroke using sensitivity encoding (SENSE). *Magn Reson Med* 2001;46:548–554.
- Golay X, Pruessmann KP, Weiger M, Crelier GR, Folkers PJM, Kollias SS, Boesiger P. PRESTO-SENSE: An ultra-fast whole brain fMRI technique. *Magn Reson Med* 2000;43:779–786.
- Jaermann T, Crelier G, Pruessmann KP, Golay X, Netsch T, Van Muiswinkel AM, Mori S, Van Zijl PC, Valavanis A, Kollias S, Boesiger P. SENSE-DTI at 3 T. *Magn Reson Med* 2004;51:230–236.